

shown in the mechanism of the Lotka model, the intermediate  $X_1$  is related to  $X_2$  through the feedback step. Even though the feedback step has indirect influence on the correlation functions through the value of the steady state, it controls the ratio of  $C_{y_2 y_2}(t)$  over  $C_{y_1 y_1}(t)$  to be  $-Ak_1/k_3$  at any time.

Including the nonlinear terms, we obtain the following eigenvalues:

$$\lambda_{1,0} = - \left( \frac{\omega_0 k_2^2 d_{11}}{8 k_3^2} \right)^{\frac{1}{2}} + i \left[ \omega_0 - \left( \frac{\omega_0 k_2^2 d_{11}}{8 k_3^2} \right)^{\frac{1}{2}} \right],$$

$$\lambda_{0,1} = \lambda_2 = -i\omega_0. \quad (3.8)$$

The effect of the nonlinear terms is to make one of the modes increase or decrease in an oscillatory fashion depending on the value of  $d_{11}$ . If  $d_{11} > 0$ , the mode with  $\lambda_{1,0}$  increases oscillatorily. It diverges as time goes to infinity. This means that we have to consider the higher order approximation to discuss the nonlinear effect. In the present paper, however, we have restricted ourselves to the first order approximation. Thus, we consider only the case of  $d_{11} < 0$ . When  $d_{11} < 0$ , the mode with  $\lambda_{1,0}$  decreases oscillatorily and the time correlation functions after long time become

$$C_{y_1 y_1}(t) = \frac{|d_{11}|}{4 \omega_0} \exp\left[i \left( \omega_0 t - \frac{\pi}{2} \right)\right],$$

$$C_{y_1 y_2}(t) = \frac{|d_{11}|}{4 k_3} \exp\left[i \left( \omega_0 t - \pi \right)\right], \quad (3.9)$$

$$C_{y_2 y_2}(t) = \frac{-Ak_1}{k_3} C_{y_1 y_1}(t).$$

The same argument for the linear system may be applied to the nonlinear case. We shall extend the present theory to

describe the dynamic phenomena of negative (and positive) metabolic control circuits<sup>12,13</sup> in the forthcoming papers.

**Acknowledgement.** This work was supported by a grant from the Basic Science Research Institute Program, Ministry of Education of Korea, 1986.

## References

1. N. G. van Kampen, *Can. J. Phys.* **19**, 551 (1961).
2. M. Suzuki, *J. Stat. Phys.* **16**, 11 (1977).
3. K. O. Han, D. J. Lee, J. M. Lee, K. J. Shin, and S. B. Ko, *Bull. Kor. Chem. Soc.* **7**, 224 (1986).
4. D. J. Lee, Unpublished.
5. J. R. Tucker and B. I. Halperin, *Phys. Rev.* **3**, 3768 (1971).
6. D. J. Lee, M. H. Ryu, and J. M. Lee, *Bull. Kor. Chem. Soc.* **6**, 295 (1985).
7. H. S. Kim and D. J. Lee, *Thesis Collection* (Chonbuk National Univ.) **26**, 494 (1984).
8. H. Risken, *The Fokker-Planck Equation* (Springer-Verlag, 1984).
9. R. Kubo, *J. Phys. Soc. Japan* **12**, 570 (1957).
10. K. J. Shin, in *Research Report for Nonlinear Phenomena and Their Theories* (Submitted to the Daewoo Foundation, 1982).
11. E. Merzbacher, *Quantum Mechanics* (John-Wiley, 1970).
12. N. MacDonald, *J. Theor. Biology* **65**, 727 (1977).
13. D. Allwright, *J. Math. Biology* **4**, 363 (1977).
14. *Selected Papers on Noise and Stochastic Processes*, ed. N. Wax (Dover, 1954).
15. P. Glansdorff and I. Prigogine, *Thermodynamic Theory of Structure, Stability and Fluctuations* (Wiley-Interscience, 1971).

## The pH Dependence of Metal Tetrakis (4-sulfonato-phenyl) porphine Structure Probed by Raman Spectroscopy

Minjoong Yoon

*Department of Chemistry, Chungnam National University, Chungnam 300-31*

Jae-Rim Chang and Dongho Kim\*

*Optics Lab., Korea Standards Research Institute, Daedok Science Town, Chungnam 300-31*

*Received October 28, 1987*

The pH dependence studies of Raman spectra are reported for water-soluble free-base, Zn, Co and Cu tetrakis (4-sulfonato-phenyl) porphine in pH 4, pH 7 and pH 13.9 aqueous solution. For free base porphine, the substantial differences are found in absorption and Raman spectra between pH 4 and pH 7 or pH 10 aqueous solutions due to the protonation at low pH. For Zn and Co porphyrins, the hydrolysis equilibrium constants are obtained by spectrophotometric titration experiments. The consistent shifts in Raman frequencies are found at high pH due to the hydrolysis. For Cu porphyrins, instead of hydrolysis the aggregation effect is detected at high pH through the absorption and Raman studies.

## Introduction

For many years, the porphyrin has been one of the central

interests in the photochemistry in view of its important roles in photosynthesis<sup>1,2</sup> and its potential utility as sensitizer in photochemical system for solar-energy conversion.<sup>3</sup> Water

-soluble porphyrins are suitable for *in vitro* studies such as visible-light-induced H<sub>2</sub> evolution from water, as has been demonstrated recently with the ZnTMPyP\*<sup>4</sup>, the solubility of porphyrins in aqueous media is enhanced by introduction of ionic groups such as SO<sub>3</sub><sup>-</sup>, CO<sub>2</sub><sup>2-</sup>, -O<sup>-</sup>, -N(CH<sub>3</sub>)<sub>3</sub><sup>+</sup>, -NC<sub>5</sub>H<sub>5</sub><sup>+</sup> (Py) etc.<sup>5</sup> on the porphyrin macrocycle ring. Some of the compounds belonging to TPPS families have been studied here.

Resonance Raman (RR) spectroscopy has been applied extensively to the study of metalloporphyrins and heme proteins, and has provided useful information about molecular structure.<sup>6</sup> The 71 in-plane vibrations for metalloporphyrins of D<sub>4h</sub> symmetry are

$$\Gamma_{1p} = 9 A_{1g} + 8 A_{2g} + 9 B_{1g} + 9 B_{2g} + 18 E_u$$

Excitation in the Soret band (380-420 nm,  $\epsilon \approx 3 \times 10^5$ ) mainly enhances the totally symmetric in-plane modes, and nontotally symmetric modes are sometimes observed. In this sense, RR spectroscopy is a powerful tool for the selective enhancement of limited number of molecular vibrational modes via coupling with the electronic transition with which the laser excitation is in resonance.<sup>6</sup>

For the possibility of solar energy conversion, the oxidation and the reduction potentials of porphyrins are one of the important parameters. The correlation between E<sub>1/2</sub> values for the first reduction of metalloporphyrins and the corresponding free-base proton affinity (*pKa*) values was found from previous works.<sup>4</sup> And depending on the oxidation potential of metalloporphyrins, the pH range of the solution is confined for the feasibility of water oxidation using the porphyrin monocation radicals as relay species.<sup>4</sup> Thus it seems relevant to determine *pKa* values and the pH dependence of structures of water-soluble porphyrins by absorption spectra and RR spectroscopy.

## Experimental

H<sub>2</sub>TPPS, CoTPPS, CuTPPS and ZnTPPS (Midcentury Chemical Co., Posen, IL) were checked by Cary 219 UV-Vis spectrometer and used without further purification. The emission spectra were recorded by fluorometer built in our laboratory using Xe-lamp, photometer and scanning Jobin-Yvon H-20 visible monochromator. Raman spectra were obtained using Spectra Physics 165 Ar<sup>+</sup> laser via 135° backscattering from the spinning nmr cell. The scattered light from the cell was collected by *f* = 1.2 camera lens and focused onto the 1 meter McPherson 2061 monochromator with 608 MI prism disperser using *f* = 30 cm planar convex lens. A Thorn EMI 9658 photomultiplier tube, cooled to -10°C with EMI FACT MK 50III cooling system, was used as a detector. The EG&G PAR 1140 C amplifier/discriminator and 1140 photon counting system were used for photon counting. The analog signal from the photon counter was changed to digital signal by A/D converter. A computer and plotted by Roland 880 XY digital plotter.

## Results and Discussion

**pH-dependent protonation of H<sub>2</sub>(TPPS).** While the emission and the absorption spectra of free-base porphine at pH 7 and pH 10 aqueous buffers are similar, at pH 4 the substantial differences are found in the absorption and the

**Table 1. Absorption Spectra for Metallo-TPPS<sup>a</sup>**

Sample	pH	Band	B	Q(1,0), Q(0,0)
H <sub>2</sub> TPPS	pH 4	434(10)	645(1), 594(0.35)	
	pH 7	416(20)	644(0.28) <sup>b</sup> , 586(0.40), 550(0.53), 516(1)	
CoTPPS	pH 7	428(30)	575(0.37), 542(1)	
	pH 13.9	432(25)	590(0.48), 555(1)	
CuTPPS	pH 7	413(34)	574(0.16), 539(1)	
	pH 13.9	404(27)	582(0.24), 545(1)	
ZnTPPS	pH 7	421(30)	594(0.40), 555(1)	
	pH 13.9	428(30)	604(0.60), 564(1)	

<sup>a</sup> Peak wavelength in nm; numbers in parentheses are peak heights relative to Q(0,0); <sup>b</sup> At pH 7, Q bands split into Q<sub>y</sub>(0,0), Q<sub>y</sub>(1,0), Q<sub>x</sub>(0,0) and Q<sub>x</sub>(1,0) in increasing wavelength order because of symmetry change from D<sub>4h</sub> (pH 4) to D<sub>2h</sub> (pH 7).

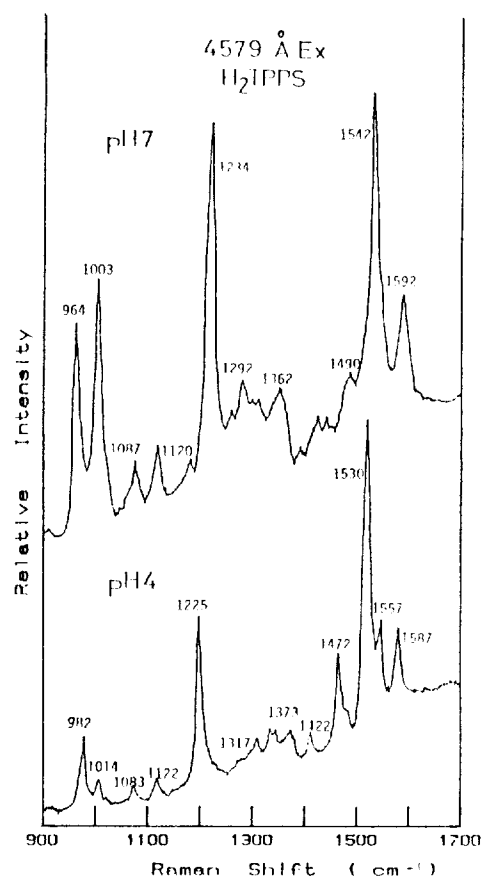
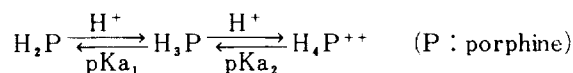


**Figure 1.** RR spectra of H<sub>2</sub>TPPS in pH 4 (bottom) and pH 7 (top) aqueous buffers obtained using the 457.9 nm Ar<sup>+</sup> line. Conditions: laser power 50 mW, slitwidth 6 cm<sup>-1</sup>, scan rate 0.5 cm<sup>-1</sup>/s.

emission spectra (Table 1). In the absorption spectra the B band (Soret band) shows a red shift from 416 nm to 434 nm with the decrease of the pH values. The *pKa*<sub>1</sub> and *pKa*<sub>2</sub> values are both 4.8. Therefore at pH 4 the major species are H<sub>4</sub>P<sup>++</sup> form.<sup>7,9</sup> The corresponding equilibria are as follows;



The most distinctive difference in absorption spectra between pH 4 and pH 7 is that at pH 7 there are four separate

**Table 2. RR frequencies and Band Assignments of Metallo-TPPS**

Sample pH Band assignments	H <sub>2</sub> TPPS		CoTPPS		CuTPPS		ZnTPPS	
	pH 4	pH 7	pH 7	pH 13.9	pH 7	pH 13.9	pH 7	pH 13.9
$\delta$ (phe), A <sub>1g</sub>	1587	1592	1595	1592	1593	1594	1594	1589
$\nu$ (C <sub>b</sub> -C <sub>b</sub> ), A <sub>1g</sub>	1530	1542	1563	1560	1556	1556	1546	1542
$\nu$ (C <sub>b</sub> -C <sub>b</sub> ), B <sub>1g</sub>	1472	1490	-	-	-	-	1492	1490
$\nu$ (C <sub>a</sub> -N), A <sub>1g</sub>	1373	1362	1368	1364	1361	1362	1349	1343
$\nu$ (C <sub>m</sub> -phe), A <sub>1g</sub>	1225	1234	1240	1237	1236	1236	1236	1233
phe $\delta$ (C-H), A <sub>1g</sub>	1014	1003	1083	1065	-	-	1084	1081
$\nu$ (phe), A <sub>1g</sub>	982	964	1010	1003	998	1000	997	987

<sup>a</sup> Notations used for band assignments are the same as those used in ref. (13) and (14).

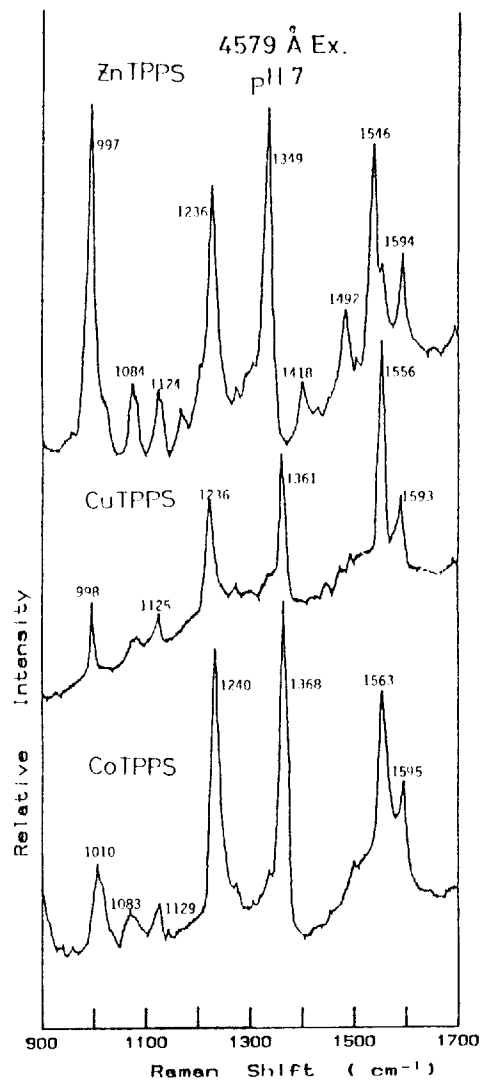


**Figure 2.** RR spectra of CoTPPS (bottom), CuTPPS (middle) and ZnTPPS (top) in pH 7 aqueous buffers obtained using the 457.9 nm Ar<sup>+</sup> line. Conditions: laser power 50 mW, slitwidth 6 cm<sup>-1</sup>, scan rate 0.5 cm<sup>-1</sup>/s.

bands around Q band (weakly allowed transition band around 500-700 nm) region compared to two separate bands in the same region at pH 4 (Table 1). The origins of these bands at pH 7 are Qx(1,0), Qx(0,0), Qy(1,0), Qy(0,0) in wavelength decreasing order (D<sub>2h</sub> symmetry).<sup>2</sup>

However when remaining two of four central nitrogens

(two nitrogens already have protons) are protonated at pH 4, the molecular symmetry is changed to D<sub>4h</sub>. Thus at pH 7 two separate bands are assigned to Q(1,0) and Q(0,0) Q(1,0) is the vibronic overtone band of Q(0,0).<sup>2</sup> In addition, the absorption spectra of free base at pH 4 is similar to those of corresponding metalloporphyrins, especially in the Q band region (Table 1). This is also due to the fact that in metalloporphyrins the molecular symmetry is D<sub>4h</sub> because two protons on the central nitrogens are substituted by a metal.<sup>2</sup>

The Raman spectra taken at pH 4 and 7 are shown in Figure 1 and Table 2 lists the Raman frequencies. At pH 4 the enhancement pattern and the frequencies are quite different, especially 982, 1225, 1373, 1530 cm<sup>-1</sup> bands compared with pH 7 or pH 10 buffers. These results stem from the core size (the distance from the center of the porphyrin to the pyrrole nitrogen) expansion and the  $\pi$ -conjugation change between the phenyl groups and the porphyrin macrocycle due to the protonation on the central nitrogens at low pH.<sup>10</sup> There is not much difference in absorption, emission and Raman spectra between pH 7 and pH 10 buffer, which indicates that the major species are the same in two different buffers.

**Structure Sensitive Bands.** Previous crystal structure studies show that core sizes are 1.949 Å, 1.981 Å and 2.045 Å for non-coordinated Co, Cu, Zn(TPP) compounds.<sup>11,12</sup> The bands which show the inverse linear relationship with the core size increase (Figure 2) are (C<sub>a</sub>-N) band around 1368 cm<sup>-1</sup> and (C<sub>b</sub>-C<sub>b</sub>) band around 1563 cm<sup>-1</sup>, by analogy to the previous works on metallo-TPP compounds.<sup>13,14</sup> The other bands do not show consistent shifts because they are mainly the vibrations involving phenyl groups.

Estimates of the core size have been derived from the observed frequencies by use of the linear relationship  $d = A - \nu/k$ , where  $\nu$  is the frequency,  $d$  is the Ct-N distance (the core size),  $k$ (cm<sup>-1</sup> Å<sup>-1</sup>) and  $A$ (Å) are the best-fit parameters. The 1560 cm<sup>-1</sup> band has been found by Stong *et al.*<sup>15</sup> to correlate with the core size with the parameter values  $A = 7.950$  Å and  $k = 262.5$  cm<sup>-1</sup> Å<sup>-1</sup>. From these values and above equation, the core sizes calculated for Co, Cu and ZnTPPS in pH 7 buffer are 1.996, 2.026 and 2.060 Å respectively. These values are higher than those of non-coordinated Co, Cu and ZnTPP compounds. However, they are close to the coordinated core size values 2.075 Å for ZnTPP(H<sub>2</sub>O) and 1.987 Å for CoTPP(pip)<sub>2</sub>.<sup>11</sup> The core size for Cu analogs is not known, and the difference between the calculated and the observed values may be due to the different phenyl group substitution on porphyrin macrocycle. From these results and previous coordination works, it is inferred that CoTPPS

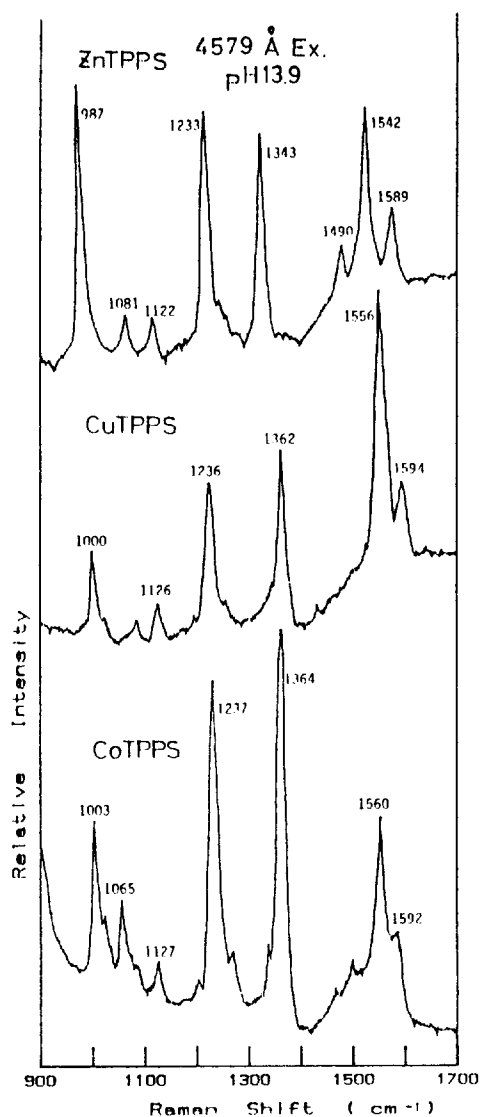


**Figure 3.** RR spectra of CoTPPS (bottom), CuTPPS (middle) and ZnTPPS (top) in pH 13.9 aqueous solutions obtained using the 457.9 nm Ar<sup>+</sup> line. Conditions: laser power 50 mW, slitwidth 6 cm<sup>-1</sup>, scan rate 0.5 cm<sup>-1</sup>/s.

exists as 6-coordinated form and Zn and CuTPPS exist as 5-coordinated form.<sup>16</sup> The axial ligands are either water or hydroxide molecules (see the following section), depending on pH.

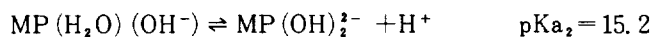
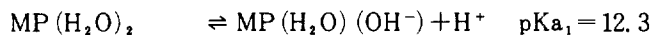
The 1368 cm<sup>-1</sup> C<sub>a</sub>-N stretching mode is sensitive to both the spin, the oxidation state of the central metal and the axial ligands.<sup>17-20</sup> This band also shows inverse linear relationship (see Table 2) as the metal size increase. However, the quantitative calculation is not made for the core size.

**pH-Dependent Equilibrium of metallo-TPPS.** Metalloporphyrins can hydrolyze by the loss of one or two protons, which is formally equivalent to the removal of a proton from a coordinated water at low acidities. The previous studies are focused on the trivalent water-soluble metalloporphyrins (eg. Fe(III), Co(III), Cr(III), Rh(III), and Mn(III)), which have *pK<sub>a1</sub>* and *pK<sub>a2</sub>* values in the range of 4-8 and 8-12 respectively.<sup>16, 21-23</sup> The quantitative analysis on hydrolysis of divalent water-soluble metalloporphyrins has not been made so far. Thus the spectrophotometric titration experiments in vari-

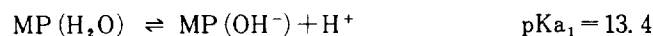
ous pH solutions are carried out to determine the hydrolysis equilibrium constants.

The results are as follows:

For Co(II):



For Zn(II):



M = metal P = porphine

The absorption spectra at pH 7 and pH 13.9 are tabulated in Table 1. The *pK<sub>a</sub>* values are higher than those of trivalent metalloporphyrins, which denote that the divalent metal oxidation state is responsible for the difficulties of the hydrolysis reaction compared to the trivalent metalloporphyrins. Raman spectra are reported to obtain the informations on the structural changes due to the hydrolysis reaction at pH 13.9 and pH 7. At pH 13.9, for ZnTPPS the percentage ratio between ZnTPPS(H<sub>2</sub>O) and ZnTPPS(OH<sup>-</sup>) species is 23%:77% and for CoTPPS the major species is CoTPPS(H<sub>2</sub>O)(OH<sup>-</sup>) (93%), the residual species existing as CoTPPS(H<sub>2</sub>O)<sub>2</sub> and CoTPPS(OH)<sub>2</sub><sup>2-</sup> forms. The Raman spectra (Figures 2, 3 and Table 2) show that the frequencies of the porphyrin skeletal modes are decrease as the pH increases. This fact is due to the structural changes and the core size differences caused by hydrolysis reaction on the axially coordinated water molecules. Probably the stronger binding by the hydroxide molecule causes the core size expansion, which results in the decrease of high frequency porphyrin skeletal modes (Table 2).<sup>13-14,17</sup> These changes are similar to those in non-water-soluble metalloporphyrin caused by ligation without spin-state changes. For CuTPPS the same experiment was attempted. However, instead of hydrolysis reaction the aggregation phenomena is detected as the pH increases. The absorption changes especially in Soret band as pH increases are opposite to those of Co and Zn TPPS's (Table 1). The absorption spectra at higher pH are similar to those when small increasing amounts of NaCl salt was added to the pH 7 aqueous solution, which was known to facilitate the aggregation reaction (salt aggregation).<sup>21</sup> And the water soluble copper porphyrins are known to be the most sensitive to aggregation reaction from previous analysis on other types of porphyrins.<sup>21</sup> The Raman spectra (Figures 2, 3 and Table 2) also show that the RR frequency shifts in CuTPPS are different from those of CoTPPS and ZnTPPS. The slight up shifts (1-2 cm<sup>-1</sup>) at high pH are due to the fact that aggregated molecules may tighten the double bond on the porphyrin macrocycle through the dimer formation.<sup>24</sup> Therefore we conclude that at higher pH CuTPPS forms aggregated molecule through the absorption and Raman spectra analysis.

**Acknowledgement.** This work was supported by the Ministry of Science and Technology fund.

## References

‡ Abbreviations used here are TPPS: tetrakis(4-sulfonatophenyl) porphine, TMPyP: tetrakis(4-methylpyridyl) porphine and TPP: tetraphenyl porphine.

1. J. Barber, ed., Topics in photosynthesis, Vols. 1-3, Elsevier, Amsterdam, (1979).

2. (a) D. Dolphin, ed., *The porphyrins*, Vols. 1-7, Academic Press, New York, (1978); (b) K. M. Smith, ed., *Porphyrins and Metalloporphyrins*, Elsevier, Amsterdam, (1975).
3. J. Darwent, P. Douglas, A. Harriman, G. Porter and M-C. Richoux, *Coord. Chem. Rev.*, **44**, 83 (1982).
4. (a) K. Kalyanasundaram and M. Grätzel, *Helv. Chim. Acta.*, **63**, 478 (1980); (b) A. Harriman, G. Porter and M-C. Richoux, *J. Chem. Soc., Faraday Trans. 2*, **77**, 833 (1981); (c) A. Harriman, G. Porter and M-C. Richoux, *J. Chem. Soc., Faraday Trans. 2*, **77**, 1939 (1981).
5. (a) R. F. Pasternack, *Ann. N. Y. Acad. Sci.*, **206**, 614 (1973); (b) R. F. Pasternack, P. R. Huber, P. Boyed, G. Engasser, L. Francesconi, E. Gibbs, P. Fasella, G. C. Ventura and L. de Hinds, *J. Am. Chem. Soc.*, **95**, 4511 (1972).
6. (a) T. G. Spiro, in: *Iron Porphyrins*, part II, ed. A. B. P. Lever and H. B. Gray, Addison-Wesley, Reading, MA, 89 (1983); (b) T. Kitagawa, Y. Ozaki and T. Kajogoku, *Adv. Biophys.*, **11**, 153 (1978); (c) J. A. Shelnut, L. D. Cheung, R. C. C. Chang, N. -T. Yu and R. H. Felton, *J. Chem. Phys.*, **66**, 3387 (1979).
7. K. Kalyanasundaram, *Inorg. Chem.*, **23**, 2453 (1984).
8. M. Krishnamurthy, *Ind. J. Chem. Part B* **15**, 964 (1977).
9. (a) A. N. Thompson and M. Krishnamurthy, *J. Inorg. Nucl. Chem.*, **41**, 1251 (1979); (b) P. Neta, *J. Phys. Chem.*, **85**, 3678 (1981).
10. N. Blom, J. Odo, K. Nakamoto and D. P. Strommen, *J. Phys. Chem.*, **90**, 2847 (1986).
11. J. L. Hoard in Ref. (2)(b) Chapt. 8, 317 and references are therein.
12. W. R. Scheidt, J. U. Mondal, C. W. Eigenbrot, A. Alder, L. J. Radonovich and J. L. Hoard, *Inorg. Chem.*, **25**, 795 (1986).
13. J. M. Burke, J. R. Kincaid and T. G. Spiro, *J. Am. Chem. Soc.*, **100**, 6077 (1978).
14. P. Stein, A. Ulman and T. G. Spiro, *J. Phys. Chem.*, **88**, 369 (1984).
15. J. D. Stong, T. G. Spiro, R. J. Kubaska and S. I. Shupack, *J. Raman spectrosc.*, **9**, 312 (1980).
16. P. Hambright in Ref. (2)(b) Chapt. 6, 233 and references are therein.
17. J. M. Burke, J. R. Kincaid, S. Peters, R. R. Gagne, J. P. Collman and T. G. Spiro, *J. Am. Chem. Soc.*, **100**, 6083 (1982).
18. S. Choi, T. G. Spiro, K. C. Langry, K. M. Smith, D. L. Budd and G. N. La Mar, *J. Am. Chem. Soc.*, **104**, 4345 (1982).
19. J. Kincaid and K. Nakamoto, *J. Inorg. Nucl. Chem.*, **37**, 85 (1975).
20. H. Oshio, T. Ama, T. Watanabe, J. Kincaid and K. Nakamoto, *Spectrochim. Acta Part A* **40A**, 863 (1984).
21. R. F. Pasternack, L. Francesconi, D. Raff and E. Spiro, *Inorg. Chem.*, **12**, 2606 (1973).
22. E. B. Fleischer, J. M. Palmer, T. S. Srivastava and A. Chatterjee, *J. Am. Chem. Soc.*, **93**, 3162 (1971).
23. E. B. Fleischer and M. Krishnamurthy, *J. Am. Chem. Soc.*, **93**, 3784 (1971).
24. J. A. Shelnut, M. M. Dobry and J. D. Satterlee, *J. Phys. Chem.*, **88**, 4980 (1984).

## Evaluation of a Radical Mechanistic Probe for NADH-dependent Horse Liver Alcohol Dehydrogenase Reactions by Computer Graphics Modeling

Sung Kee Chung\* and Daniel F. Chodosh†

\*Smith Kline & French Laboratories 1500 Spring Garden St, Philadelphia, PA 19101, Pohang  
Institute of Science & Technology, Pohang 680. Received November, 4, 1987

The feasibility of the reduction of nortricyclanone (**1**) as a chemical probe for testing the proposed radical mechanism for NAD-dependent horse liver alcohol dehydrogenase (HLADH) reactions has been examined using computer graphics modeling. The results of this study suggest that the radical ring-opening of this probe molecule may involve too substantial a geometry reorganization for the molecule to serve as a chemical probe in detecting the possible presence of the radical intermediates in the HLADH reactions. This result suggests that one should exercise caution in extrapolating results obtained from chemically based radical probes in the solution phase to the topologically constrained systems such as enzyme-substrate reactions.

The detailed description of chemical mechanism and the transition state structure for the hydrogen transfer step in the NADH-dependent alcohol dehydrogenase reactions has been a subject of continuing debate. The key mechanistic question is whether the hydrogen transfer between the coenzyme and the substrate carbonyl functionality occurs in a sin-

gle step as a hydride or in two steps as an electron followed by a hydrogen atom. The structural and kinetic data, and *in vitro* modeling information available on this enzyme-coenzyme system, while substantial, has not yet resulted in a general consensus in support of one of the proposed mechanisms.<sup>1</sup>

Definitive interpretations of various kinetic data obtained for the actual enzyme reactions have been problematic since the hydrogen transfer step is not always the rate-determining

† Present Address - Distributed Chemical Graphics, Inc. 1326 Carol Road, Meadebrook, PA19096 U. S.A.